

**\*\*DRAFT04\*\* Search for the Decay**

$$K^+ \rightarrow \pi^+ \gamma \gamma$$

**in the  $\pi^+$  Momentum Region  $P > 213 \text{ MeV}/c$**

E949 Collaboration

V.V. Anisimovsky<sup>a</sup>, A.V. Artamonov<sup>b</sup>, B. Bassalleck<sup>c</sup>,  
B. Bhuyan<sup>d,1</sup>, E.W. Blackmore<sup>e</sup>, D.A. Bryman<sup>f</sup>, S. Chen<sup>e</sup>,  
I-H. Chiang<sup>d</sup>, I.-A. Christidi<sup>g</sup>, P.S. Cooper<sup>h</sup>, M.V. Diwan<sup>d</sup>,  
J.S. Frank<sup>d</sup>, T. Fujiwara<sup>i</sup>, J. Hu<sup>e</sup>, A.P. Ivashkin<sup>a</sup>, D.E. Jaffe<sup>d</sup>,  
S. Kabe<sup>j</sup>, S.H. Kettell<sup>d</sup>, M.M. Khabibullin<sup>a</sup>,  
A.N. Khotjantsev<sup>a</sup>, P. Kitching<sup>k</sup>, M. Kobayashi<sup>j</sup>,  
T.K. Komatsubara<sup>j</sup>, A. Konaka<sup>e</sup>, A.P. Kozhevnikov<sup>b</sup>,  
Yu.G. Kudenko<sup>a</sup>, A. Kushnirenko<sup>h,2</sup>, L.G. Landsberg<sup>b</sup>,  
B. Lewis<sup>c</sup>, K.K. Li<sup>d</sup>, L.S. Littenberg<sup>d</sup>, J.A. Macdonald<sup>e,3</sup>,  
J. Mildenerger<sup>e</sup>, O.V. Mineev<sup>a</sup>, M. Miyajima<sup>l</sup>, K. Mizouchi<sup>i</sup>,  
V.A. Mukhin<sup>b</sup>, N. Muramatsu<sup>m</sup>, T. Nakano<sup>m</sup>, M. Nomachi<sup>n</sup>,  
T. Nomura<sup>i</sup>, T. Numao<sup>e</sup>, V.F. Obraztsov<sup>b</sup>, K. Omata<sup>j</sup>,  
D.I. Patalakha<sup>b</sup>, S.V. Petrenko<sup>b</sup>, R. Poutissou<sup>e</sup>,  
E.J. Ramberg<sup>h</sup>, G. Redlinger<sup>d</sup>, T. Sato<sup>j</sup>, T. Sekiguchi<sup>j</sup>,  
T. Shinkawa<sup>o</sup>, R.C. Strand<sup>d</sup>, S. Sugimoto<sup>j</sup>, Y. Tamagawa<sup>l</sup>,

R. Tschirhart<sup>h</sup>, T. Tsunemi<sup>j,4</sup>, D.V. Vavilov<sup>b</sup>, B. Viren<sup>d</sup>,  
N.V. Yershov<sup>a</sup>, Y. Yoshimura<sup>j</sup>, T. Yoshioka<sup>j,5</sup>

<sup>a</sup>*Institute for Nuclear Research RAS, 60 October Revolution Pr. 7a, 117312  
Moscow, Russia*

<sup>b</sup>*Institute for High Energy Physics, Protvino, Moscow Region, 142 280, Russia*

<sup>c</sup>*Department of Physics and Astronomy, University of New Mexico, Albuquerque,  
NM 87131, USA*

<sup>d</sup>*Brookhaven National Laboratory, Upton, NY 11973, USA*

<sup>e</sup>*TRIUMF, 4004 Wesbrook Mall, Vancouver, British Columbia, Canada V6T 2A3*

<sup>f</sup>*Department of Physics and Astronomy, University of British Columbia,  
Vancouver, British Columbia, Canada V6T 1Z1*

<sup>g</sup>*Department of Physics and Astronomy, Stony Brook University, Stony Brook,  
NY 11794, USA*

<sup>h</sup>*Fermi National Accelerator Laboratory, Batavia, IL 60510, USA*

<sup>i</sup>*Department of Physics, Kyoto University, Sakyo-ku, Kyoto 606-8502, Japan*

<sup>j</sup>*High Energy Accelerator Research Organization (KEK), Oho, Tsukuba, Ibaraki  
305-0801, Japan*

<sup>k</sup>*Centre for Subatomic Research, University of Alberta, Edmonton, Canada T6G  
2N5*

<sup>l</sup>*Department of Applied Physics, Fukui University, 3-9-1 Bunkyo, Fukui, Fukui  
910-8507, Japan*

<sup>m</sup>*Research Center for Nuclear Physics, Osaka University, 10-1 Mihogaoka,  
Ibaraki, Osaka 567-0047, Japan*

<sup>n</sup>*Laboratory of Nuclear Studies, Osaka University, 1-1 Machikaneyama, Toyonaka,  
Osaka 560-0043, Japan*

---

**Abstract**

We have performed a search for the  $K^+ \rightarrow \pi^+ \gamma \gamma$  decay at rest in the kinematic region with  $\pi^+$  momentum close to the end point. No events were observed, and a 90% confidence-level upper limit on the partial branching ratio  $B(K^+ \rightarrow \pi^+ \gamma \gamma, P > 213 \text{ MeV}/c)$  is determined to be  $8.3 \times 10^{-9}$  under the assumption of the chiral perturbation theory including next-to-leading order “unitarity” corrections. Improved limits were set on the rates of  $K^+ \rightarrow \pi^+ X^0$  and  $X^0 \rightarrow \gamma \gamma$ , where  $X^0$  is a hypothetical short-lived neutral particle with mass smaller than  $100 \text{ MeV}/c^2$ . The same data were used to determine an upper limit on the  $K^+ \rightarrow \pi^+ \gamma$  branching ratio to  $2.3 \times 10^{-9}$ .

*Key words:* kaon rare decay, chiral perturbation theory, unitarity corrections, noncommutative standard models

*PACS:* 13.20.Eb, 12.39.Fe, 11.10.Nx

---

---

<sup>1</sup> Also at the Department of Physics, University of Delhi, Delhi 110007, India.

Present address: Department of Physics and Astronomy, University of Victoria, Victoria, British Columbia, Canada V8W 3P6.

<sup>2</sup> Present address: Institute for High Energy Physics, Russia.

<sup>3</sup> Deceased.

<sup>4</sup> Present address: Research Center for Nuclear Physics, Osaka University, Japan.

<sup>5</sup> Present address: International Center for Elementary Particle Physics, University of Tokyo, Tokyo 113-0033, Japan.

We report the results of a new search for the rare decay  $K^+ \rightarrow \pi^+ \gamma \gamma$  in the  $\pi^+$  momentum region  $P > 213$  MeV/ $c$  from the E949 experiment [1] at the Alternating Gradient Synchrotron (AGS) of Brookhaven National Laboratory (BNL). The first observation of the decay in the  $\pi^+$  momentum region 100 - 180 MeV/ $c$  was reported [2] by the BNL-E787 experiment with a partial branching ratio of  $B(K^+ \rightarrow \pi^+ \gamma \gamma, 100 \text{ MeV}/c < P < 180 \text{ MeV}/c) = (6.0 \pm 1.5(stat) \pm 0.7(syst)) \times 10^{-7}$ . In the  $\pi^+$  momentum region greater than 215 MeV/ $c$  no  $K^+ \rightarrow \pi^+ \gamma \gamma$  decay was observed and, assuming the phase-space kinematic distribution, a 90% confidence-level (C.L.) upper limit of  $5.0 \times 10^{-7}$  was set to the total branching ratio. It was concluded that, to the study of the rare decay  $K^+ \rightarrow \pi^+ \nu \bar{\nu}$  [3], the contribution of the  $K^+ \rightarrow \pi^+ \gamma \gamma$  background should be negligible.

In an effective-field approach to low energy QCD called chiral perturbation theory (ChPT) [4], there is no tree-level  $O(p^2)$  contribution to  $K^+ \rightarrow \pi^+ \gamma \gamma$  or the neutral counterpart  $K_L^0 \rightarrow \pi^0 \gamma \gamma$ ; the leading contributions start at  $O(p^4)$  [5]. For  $K^+ \rightarrow \pi^+ \gamma \gamma$ , both the branching ratio and the  $\pi^+$  spectrum shape are sensitive to the undetermined coupling-constant  $\hat{c}$ . The next-to-leading order includes one-loop “unitarity” corrections, which are deduced from an empirical fit of the decay amplitude of  $K^+ \rightarrow \pi^+ \pi^+ \pi^-$  and contain the same constant  $\hat{c}$ , and predicts the  $\pi^+$  spectrum with a slightly different shape (Fig. 1). The contribution of vector-meson exchange is expected to be negligible compared to unitarity corrections [6]. The measured  $\pi^+$  spectrum of E787, Fig. 2 in [2], was consistent both with unitarity corrections ( $\hat{c} = 1.8 \pm 0.6$ ) and without unitarity corrections ( $\hat{c} = 1.6 \pm 0.6$ ); the E787 data preferred the inclusion of the corrections but were not conclusive. For  $K_L^0 \rightarrow \pi^0 \gamma \gamma$ , the amplitude at  $O(p^4)$  is determined unambiguously but the measured branching

ratio,  $(1.41 \pm 0.12) \times 10^{-6}$  [7], is twice as large as predicted; the vector meson contribution (sometimes parametrized by an effective coupling constant  $a_v$ ) is considered to be important to this decay [8].

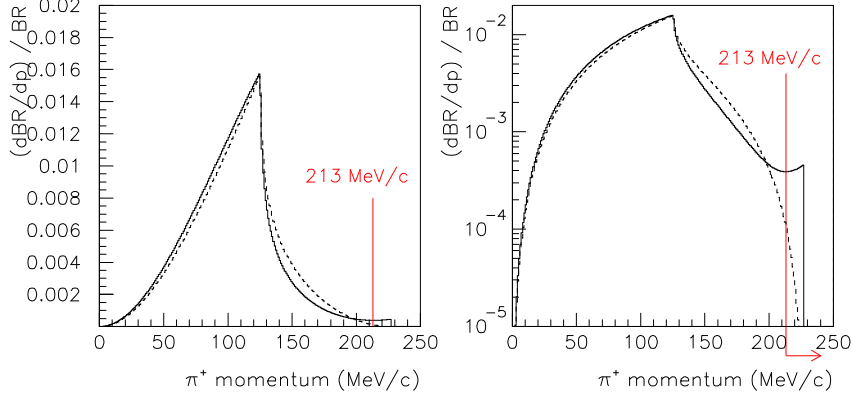


Fig. 1. Predictions for the  $\pi^+$  momentum for  $\hat{c} = 1.8$  including unitarity corrections (solid line) and for  $\hat{c} = 1.6$  without the corrections (dashed line), respectively, in the linear (left) and logarithmic (right) scales. The ratio of the partial branching ratio in the kinematic region  $P > 213$  MeV/c, indicated by the arrow, to the total branching ratio is  $5.77 \times 10^{-3}$  in the former and  $5.15 \times 10^{-4}$  in the latter.

One of the consequences of the unitarity corrections to  $K^+ \rightarrow \pi^+ \gamma \gamma$  is a nonzero amplitude in the kinematic region close to the end point of  $P = 227$  MeV/c (the two-photon invariant mass  $m_{\gamma\gamma} = 0$  MeV/c<sup>2</sup>), as shown in Fig. 1. The partial branching ratio  $B(K^+ \rightarrow \pi^+ \gamma \gamma, P > 213 \text{ MeV}/c)$ , corresponding to  $m_{\gamma\gamma} < 108 \text{ MeV}/c^2$ , is predicted to be  $6.10^{+0.16}_{-0.12} \times 10^{-9}$  for  $\hat{c} = 1.8 \pm 0.6$  including unitarity corrections and  $0.49^{+0.23}_{-0.18} \times 10^{-9}$  for  $\hat{c} = 1.6 \pm 0.6$  without the corrections. The former is one order of magnitude larger than the latter, and is within reach of E949. The kinematic region close to the end point in  $K_L^0 \rightarrow \pi^0 \gamma \gamma$  is known to be crucial to understand the CP-conserving component to the  $K_L^0 \rightarrow \pi^0 e^+ e^-$  decay, but experimental results on  $a_v$  [9,10] are inconsistent and their theoretical interpretations are controversial (see [11]).

E949 is primarily designed to measure the decay  $K^+ \rightarrow \pi^+ \nu \bar{\nu}$  [12]. The AGS delivered kaons of 710 MeV/ $c$  to the experiment at a rate of  $9 \times 10^6$  per 2.2-s spill. Kaons, detected and identified by Čerenkov, tracking, and energy-loss counters, were slowed by a Be degrader, and came to rest and decayed in a scintillating-fiber target. Fig. 2 shows a diagram of the apparatus. Measurements of charged decay products were made using the target, a central drift chamber, and a cylindrical range stack (RS) composed of 17 layers of 2-cm thick plastic scintillator with two embedded layers of tracking chambers. The pion from the  $K^+ \rightarrow \pi^+ \gamma \gamma$  decay was identified by comparing the measurements of momentum, range (equivalent cm of plastic scintillator,  $R$ ), and kinetic-energy ( $E$ ), and by observation of the  $\pi^+ \rightarrow \mu^+ \rightarrow e^+$  decay sequence at rest in the RS using 500-MHz flash-ADC waveform digitizers [13]. Sets of thin trigger counters (“I” and “T” in Fig. 2) surrounding the drift chamber defined the fiducial region, and thin counters surrounding the RS suppressed the muons from  $K^+ \rightarrow \mu^+ \nu$  and  $K^+ \rightarrow \mu^+ \nu \gamma$  decays whose range is long. The trigger requirement of a sufficient time delay ( $\geq 1.5$  ns) between the Čerenkov and I counter signals ensured that the kaons had decayed at rest in the target. A hermetic calorimeter system surrounded the central region; the photons from  $K^+ \rightarrow \pi^+ \gamma \gamma$  were detected in a lead/scintillator sandwich barrel detector (BV) surrounding the RS, while two endcap calorimeters and other detectors were used for detecting extra particles. A solenoid surrounding the BV provided a 1 T magnetic field along the beam line.

The beam and apparatus in E949, as well as the proton beam intensity from the AGS, were improved over those used in E787 [14] for the  $K^+ \rightarrow \pi^+ \gamma \gamma$  study, which was performed in 1991. The kaon beam line [15], which incorporated two stages of particle separation, reduced pion contamination while

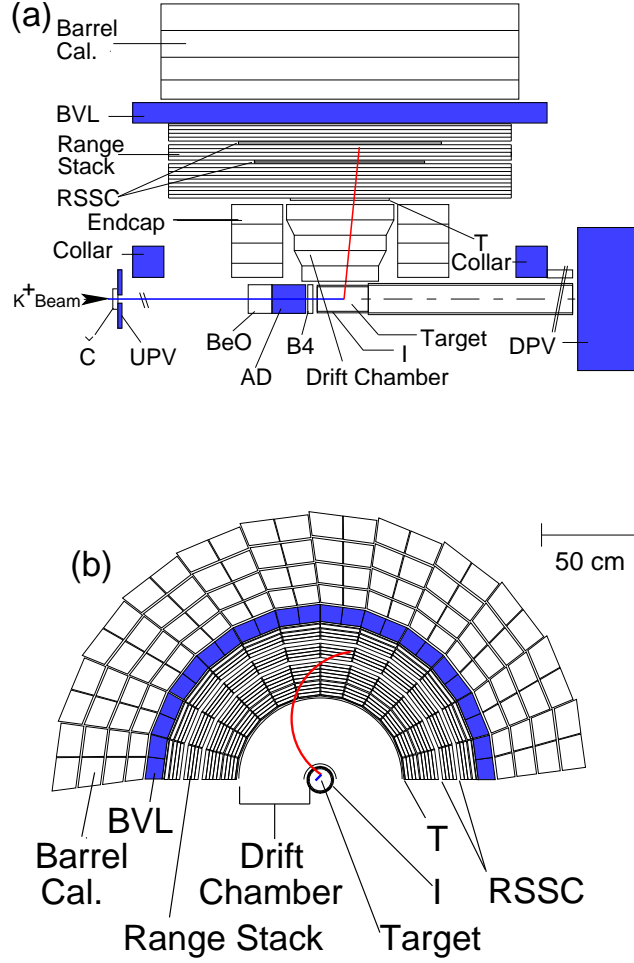


Fig. 2. Schematic side (a) and end (b) views of the upper half of the E949 detector. Č: Čerenkov counter; B4: energy-loss counters; I and T: inner and outer trigger scintillation counters; RSSC: RS straw-tube tracking chambers. New or upgraded subsystems for E949 (shaded) included the barrel veto liner (BVL), collar, upstream photon veto (UPV), active degrader (AD), and downstream photon veto (DPV). In addition, the outer trigger detectors and other trigger and electronics systems were improved in E949.

increasing kaon acceptance. The target, central drift chamber, and RS tracking chambers were replaced by a new target consisting of 0.5-cm square fibers, a new low-mass drift chamber [16], and straw-tube chambers, respectively. One third of the RS scintillation counters were replaced to increase the light output. A new photon detector, the barrel veto liner (BVL), was installed to add

2.3 radiation lengths of lead/scintillator sandwich material to the BV. The endcaps were replaced by new fully-active detectors consisting of undoped-CsI crystals [17] with significantly increased light output, and both the target and endcaps were read out using 500-MHz CCD waveform digitizers [18] to improve timing and double pulse resolution. Additional ancillary photon veto systems [19] and an LED flasher system to aid in the RS energy calibration were also introduced.

The new data were acquired in 2002, and the total exposure of kaons entering the target available for the  $K^+ \rightarrow \pi^+ \gamma \gamma$  study in E949 was  $N_K = 1.2 \times 10^{12}$ . The trigger required a kaon decay at rest, followed by a  $\pi^+$  track which came to rest in the RS and by coincident activity due to electromagnetic showers in both the BVL and BV, and no extra particles in the endcap or RS counters. The RS counter where the  $\pi^+$  track came to rest, called the “stopping counter”, was required to be in the 15th or 16th layer in order to suppress  $\pi^+$  tracks from the  $K^+ \rightarrow \pi^+ \pi^0$  decay ( $K_{\pi 2}$ ) with  $P = 205$  MeV/ $c$ ,  $R = 30.4$  cm, and  $E = 108$  MeV. An improved trigger system [20] of E949, including a programmable trigger board, allowed more efficient running and reduced deadtimes. A total of  $1.1 \times 10^7$  events met the trigger requirements.

The signature of  $K^+ \rightarrow \pi^+ \gamma \gamma$  was a kaon decay at rest with a  $\pi^+$  track in the RS in the kinematic region above the  $K_{\pi 2}$  monochromatic peak and with photons reconstructed in the BVL and BV calorimeters. The accepted  $\pi^+$  tracks in  $213 \text{ MeV}/c < P < 234 \text{ MeV}/c$ ,  $33.5 \text{ cm} < R < 41.3 \text{ cm}$ , and  $116 \text{ MeV} < E < 135 \text{ MeV}$  were 3.3, 2.3, and 2.6 standard-deviations above the  $K_{\pi 2}$  peak, respectively. Due to improvements in the kinematic reconstruction, the search region was enlarged over E787 ( $P > 215 \text{ MeV}/c$  and a constrained kinematic fit for consistency with  $K^+ \rightarrow \pi^+ \gamma \gamma$ ) [2]. The timing and energy



$(E_\gamma)$  of the photons were determined by grouping adjacent hit modules in BV and BVL to identify isolated photon showers (“clusters”). The hit position in each module along the beam axis ( $z$ ) was calculated from the end-to-end time and energy differences; the azimuthal angle ( $\phi$ ) of the hit position was determined by which module was hit. The location of the photon shower in  $z$  and  $\phi$  was obtained by an energy-weighted average of the hit positions and was used, in conjunction with the kaon-decay vertex position in the target, to determine the polar and azimuthal angles of the photon to the  $\pi^+$  track ( $\theta_{\pi^+\gamma}$  and  $\phi_{\pi^+\gamma}$ ). Since the opening angle between two photons from  $K^+ \rightarrow \pi^+\gamma\gamma$  gets narrower for the events whose  $\pi^+$  momentum is close the kinematic end point, the two photons of about one half of the signal events form a single cluster in BVL and BV within their limited position-resolutions; the events with exactly one or two clusters were therefore accepted in the offline analysis. The highest-energy cluster should satisfy  $50 \text{ MeV} < E_\gamma < 320 \text{ MeV}$ ,  $\theta_{\pi^+\gamma} > 155^\circ$ , and  $\phi_{\pi^+\gamma} > 155^\circ$ . The energy of the lower-energy cluster, if exists, should be at least 10 MeV.

There were three background sources from kaon decays at rest. The first one (“mismeasured”) is the  $K_{\pi^2}$  decay due to mismeasurements of the  $\pi^+$  and the two photons, including detection inefficiency of the softer of the photons from  $\pi^0$  if exactly one cluster is reconstructed. The second one (“overlap”) is the  $K_{\pi^2}$  decay due to the disappearance of the softer photon through overlap with the  $\pi^+$  track in the RS; the reconstructed kinetic energy of such tracks could be incorrectly measured due to additional energy deposited in the scintillators by the overlapping photon. The third one (“mudecay”) is the kaon decays with a muon, misidentified as  $\pi^+$ , and with some photons in the final state, such as  $K^+ \rightarrow \mu^+\nu\gamma$  and  $K^+ \rightarrow \pi^0\mu^+\nu$  decays, as well as the  $K_{\pi^2}$  decay whose  $\pi^+$

decays in flight to  $\mu^+$  in the detector. The  $K_{\pi 2}$  decay in flight in the beam line before the kaon comes to rest (“DIF”), if the  $\pi^+$  momentum is Lorentz-boosted and satisfies the conditions for  $K^+ \rightarrow \pi^+ \gamma \gamma$ , is the background source from the incident beam particles. Other beam-related backgrounds (e.g. multiple beam particles into the detector) were found to negligible.

These backgrounds were studied from the data by imposing offline selection criteria (“cuts”). For the background sources from kaon decays at rest, the cuts on the accepted region of the  $\pi^+$  momentum, range and kinetic energy were valid. The cuts on the invariant mass of two photons (to reject events with  $m_{\gamma\gamma} > 100 \text{ MeV}/c^2$ ), on extra activity (to reject events with activity not associated with the  $\pi^+$  and the candidate signal photons <sup>6</sup>), and on the photon clusters (to reject events with two photons from a  $\pi^0$  which hit the same or adjacent modules in BVL and BV and form a single cluster <sup>7</sup>) [21] were imposed to remove the mismeasured background. The  $dE/dx$  cuts in the RS (to reject events with a RS counter in which the measured energy was larger than expected from the reconstructed range in that counter) were imposed to remove the overlap background [21]. The cuts on the relation between the range measured in the RS and the momentum measured in the drift chamber as well as the cuts on the  $\pi^+ \rightarrow \mu^+ \rightarrow e^+$  decay sequence, recorded in the RS stopping counter, were imposed to remove the muon decay background. The

---

<sup>6</sup> The extra activity was identified in the various subsystems, including the RS, as hits in the counters in coincidence with the  $\pi^+$  track within a few ns and with energy above a threshold of typically  $\sim 1 \text{ MeV}$ .

<sup>7</sup> Due to the kinematics of  $K_{\pi 2}$  and subsequent  $\pi^0 \rightarrow \gamma\gamma$  decays, the two photons must hit the modules at different  $z$  positions along the beam axis. An event was rejected if the maximum discrepancy among the  $z$ -position measurements in the modules of the cluster was larger than 113 cm.

DIF background was studied by the cuts on the delay ( $\geq 2$  ns) between the  $\pi^+$  time and the  $K^+$  time measured in the target and the cuts on the timing between the  $\pi^+$  in the RS and the  $K^+$  in the Čerenkov counter.

In studying these backgrounds, two independent sets of cuts were established for each background source. We inverted at least one of these cuts on the events in order to enhance the background collected by the trigger as well as to prevent candidate events from being examined before the background studies were completed. In order to avoid contamination from other background sources, all the offline cuts except for those being established were imposed on the data. Possibilities of a correlation between two sets of cuts and of a biased estimate of the effectiveness of the cuts, the level of signal acceptance as a function of cut severity, the check of the observed background levels near but outside the signal region in comparison with the predicted background rate, etc. were studied [22] by following the procedures developed through the  $K^+ \rightarrow \pi^+ \nu \bar{\nu}$  analysis in E949 and E787 [12,23]. Table 1 summarizes the background levels measured with the final analysis cuts and the two sets of cuts for studying each background source. In total,  $0.197 \pm 0.070$  background events were expected in the signal region.

The acceptance ( $A$ ) and the single event sensitivity ( $SES$ ) for  $K^+ \rightarrow \pi^+ \gamma \gamma$  in the kinematic region  $P > 213$  MeV/ $c$  were derived from the acceptance factors in Table 2, the total kaon exposure  $N_K = 1.2 \times 10^{12}$ , and the  $K^+$  stop efficiency, which is the fraction of kaons entering the target that came to rest and was measured with the  $K_{\pi 2}$  events collected by the same trigger, of  $0.754 \pm 0.024$ . We obtained  $A = (2.99 \pm 0.07) \times 10^{-4}$  and  $SES = (3.72 \pm 0.14) \times 10^{-9}$  for  $\hat{c} = 1.8$  including unitarity corrections and  $A = (1.18 \pm 0.04) \times 10^{-4}$  and  $SES = (9.40 \pm 0.45) \times 10^{-9}$  for  $\hat{c} = 1.6$  without the corrections. The

Source	background level	two sets of cuts	
kaon decays at rest: $K_{\pi 2}$ , $\mu^+\nu\gamma$ , $\pi^0\mu^+\nu$			
mismeasured	$0.017 \pm 0.006$	$\pi^+$ accepted region ( $P,R,E$ )	$m_{\gamma\gamma}$  extra activity  photon clusters
overlap	$0.065 \pm 0.065$	$\pi^+$ accepted region ( $P,R$ )	$dE/dx$
mudecay	$0.090 \pm 0.020$	$\pi^+$ accepted region ( $P,R,E$ )  range-momentum relation	$\pi^+ \rightarrow \mu^+ \rightarrow e^+$
incident beam particles			
DIF	$0.025 \pm 0.014$	delay in the target	RS - Č timing

Table 1

Expected background levels in the signal region and the two sets of cuts for studying each background source. The total background level in the analysis was expected to be  $0.197 \pm 0.070$  in the signal region.

former sensitivity was below the predicted branching ratio of  $6.10 \times 10^{-9}$ , giving an expectation of 1.6 events. In order to verify that the sensitivity estimations were correct, the sample of  $K^+ \rightarrow \mu^+\nu$  decays accumulated by a calibration trigger was analyzed. The measured branching ratio of  $0.628 \pm 0.020$  was consistent with the Particle Data Group value [7], which indicated that the systematic uncertainty in this study is small.

After imposing all analysis cuts, no events were observed in the signal region

(Fig. 3). The group of 74 events around  $R = 32$  cm and  $E = 110$  MeV <sup>8</sup> are due to the  $K_{\pi 2}$  background. Taking 2.24 events instead of zero according to the unified approach [24,7] with the background contribution of 0.197 events, we set a 90% C.L. upper limit on the partial branching ratio  $B(K^+ \rightarrow \pi^+ \gamma \gamma, P > 213 \text{ MeV}/c)$  as  $8.3 \times 10^{-9}$  for  $\hat{c} = 1.8$  including unitarity corrections and  $2.1 \times 10^{-8}$  for  $\hat{c} = 1.6$  without the corrections. The systematic uncertainty was not taken into consideration in deriving the limits. For the purpose of comparison with the previous E787 results, a 90% C.L. upper limit for the total  $K^+ \rightarrow \pi^+ \gamma \gamma$  branching ratio assuming the phase-space distribution was calculated; the limit  $6.0 \times 10^{-8}$  is 8.3 times better than the same limit in E787 ( $5.0 \times 10^{-7}$ ).

The data also set limits on sequential decays in the form  $K^+ \rightarrow \pi^+ X^0$ ,  $X^0 \rightarrow \gamma \gamma$ , where  $X^0$  is any short-lived neutral particle with a mass  $m_{X^0}$  smaller than 100 MeV/ $c$  decaying into two photons. Fig. 4 shows the limit as a function of  $m_{X^0}$  for different lifetimes.

The data described above were used to set a 90% C.L. upper limit on the branching ratio for the  $K^+ \rightarrow \pi^+ \gamma$  decay, which is forbidden by angular-momentum conservation and by gauge invariance but is allowed in noncommutative standard models [25]. The signature of  $K^+ \rightarrow \pi^+ \gamma$  was a two-body decay of a kaon at rest with a 227-MeV/ $c$   $\pi^+$  track in the RS and a 227-MeV photon emitted directly opposite to it and observed as a single cluster in the BVL and BL calorimeter. The same trigger, event reconstruction, offline selection criteria (and background levels) as in the study of  $K^+ \rightarrow \pi^+ \gamma \gamma$

---

<sup>8</sup> These values are slightly larger than those expected for the  $K_{\pi 2}$  decay, because the stopping-layer requirement in the trigger collected the  $K_{\pi 2}$  events whose range and energy were measured to be larger in the RS.

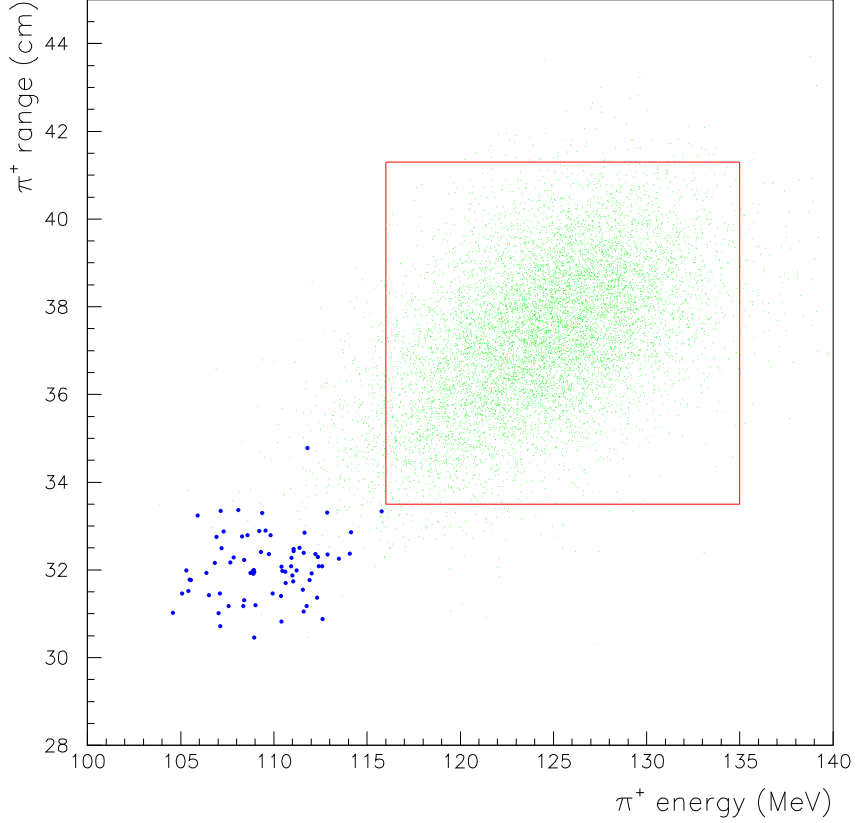


Fig. 3. Range vs. kinetic energy plot of the events with all analysis imposed. The box indicates the signal region for the  $K^+ \rightarrow \pi^+ \gamma \gamma$  decay. The dark points represent the data. The simulated distribution of expected events from  $K^+ \rightarrow \pi^+ \gamma \gamma$  for  $\hat{c} = 1.8$  including unitarity corrections is indicated by the light dots.

were available to the search. The previous limit from the E787 study was  $3.6 \times 10^{-7}$  [21], which was performed in 1996 and 1997 with a highly-prescaled trigger with relaxed conditions resulting in the total exposure of kaons to be  $6.7 \times 10^8$ . The new limit from E949, using the acceptance for  $K^+ \rightarrow \pi^+ \gamma$  of  $(1.08 \pm 0.02) \times 10^{-3}$ , is  $2.3 \times 10^{-9}$ .

The results from this study cannot confirm nor rule out the unitarity corrections of ChPT, but the upper limits obtained are the tightest yet achieved on  $K^+ \rightarrow \pi^+ \gamma \gamma$ ,  $K^+ \rightarrow \pi^+ X^0$ , and  $K^+ \rightarrow \pi^+ \gamma$  decays. The analysis, which was limited by the total exposure of kaons available at the data taking in

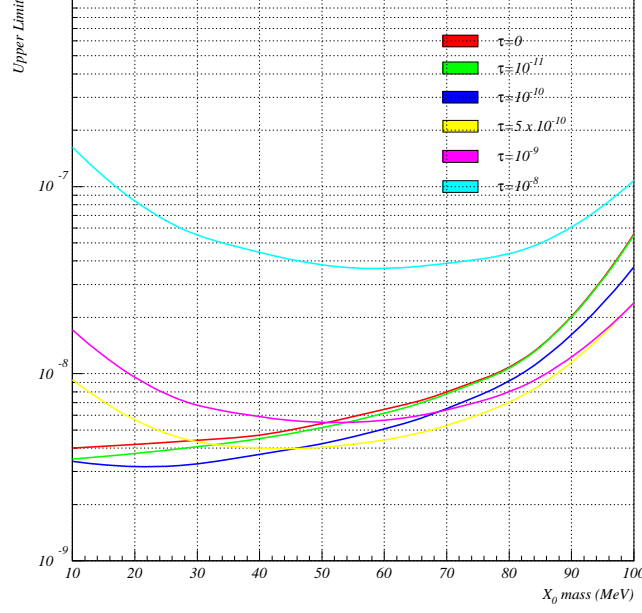


Fig. 4. The 90% C.L. upper limits for the branching ratio of  $K^+ \rightarrow \pi^+ X^0$ ,  $X^0 \rightarrow \gamma\gamma$  for different  $X^0$  lifetimes ( $\tau$ ) in seconds as a function of  $X^0$  mass.

2002, has proved that the experiment with kaon decays at rest is suitable to study  $K^+ \rightarrow \pi^+ \gamma\gamma$  in the  $\pi^+$  momentum region close to the end point. The possibility to observe signal events of  $K^+ \rightarrow \pi^+ \gamma\gamma$  in the kinematic region, if the ChPT including unitarity corrections is correct, gives further impetus for additional data collection.

## Acknowledgements

We gratefully acknowledge the dedicated effort of the technical staff supporting E949 and of the Brookhaven AGS Department. This research was supported in part by the U.S. Department of Energy, the Ministry of Education, Culture, Sports, Science and Technology of Japan through the Japan-U.S. Cooperative Research Program in High Energy Physics and under Grant-in-Aids for Scientific Research, the Natural Sciences and Engineering Research Council and

the National Research Council of Canada, the Russian Federation State Scientific Center Institute for High Energy Physics, and the Ministry of Science and Education of the Russian Federation.



Acceptance factors	UC	w/o UC	samples
Trigger	0.0666	0.0435	MC
Trigger-counter efficiency	0.936	0.936	$K_B$
charged-track reconstruction	0.996	0.996	$K_{\mu 2}$
$\pi^+$ fiducial cuts	0.898	0.626	MC
$\pi^+$ stop without nuclear interaction or decay-in-flight	0.492	0.578	MC
$dE/dx$ and kinematic cuts	0.537	0.537	$K_{\pi 2}, \pi_{scat}$
$\pi^+ \rightarrow \mu^+ \rightarrow e^+$ cuts	0.349	0.349	$\pi_{scat}$
$\gamma$ reconstruction and fiducial cuts	0.530	0.492	MC, $K_{\pi 2}$ ,
Extra activity cuts	0.216	0.173	MC, $K_{\pi 2}$ ,
Other cuts on beam and target	0.507	0.507	$K_{\mu 2}$
Total acceptance	$2.99 \times 10^{-4}$	$1.18 \times 10^{-4}$	

Table 2

Acceptance factors for the  $K^+ \rightarrow \pi^+ \gamma \gamma$  decay in the kinematic region  $P > 213$  MeV/c, for  $\hat{c} = 1.8$  including unitarity corrections (“UC”) and for  $\hat{c} = 1.6$  without the corrections (“w/o UC”), and the samples used to determine them. “MC” in the rightmost column means the sample generated by Monte Carlo simulation. “ $K_B$ ”, “ $K_{\mu 2}$ ”, “ $K_{\pi 2}$ ”, and “ $\pi_{scat}$ ” mean the data samples of kaons entering the target,  $K^+ \rightarrow \mu^+ \nu$  decays,  $K_{\pi 2}$  decays, and scattered beam pions, respectively; these samples were accumulated by calibration triggers simultaneous to the collection of signal candidates.

## References

- [1] B. Bassalleck *et al.*, E949 Proposal, BNL-67247, TRI-PP-00-06 (1999), [<http://www.phy.bnl.gov/e949/>] .
- [2] P. Kitching *et al.*, Phys. Rev. Lett. **79**, 4079 (1997).
- [3] A.J. Buras, F. Schwab, and S. Uhlig, hep-ph/0405132, and references therein.
- [4] J.F. Donoghue, E. Golowich, and B.R. Holstein, *Dynamics of the Standard Model* (Cambridge University Press, Cambridge, 1992), and references therein.
- [5] G. Ecker, A. Pich, and E. de Rafael, Phys. Lett. **B189**, 363 (1987); Nucl. Phys. **B303**, 665 (1988); L. Cappiello and G. D'Ambrosio, Nuovo Cimento **A99**, 155 (1988).
- [6] G. D'Ambrosio and J. Portolés, Phys. Lett. **B389**, 770 (1996); Nucl. Phys. **B492**, 417 (1997).
- [7] Particle Data Group, S. Eidelman *et al.*, Phys. Lett. **B592**, 1 (2004).
- [8] E.g., G. Ecker, A. Pich, and E. de Rafael, Phys. Lett. **B237**, 481 (1990); A.G. Cohen, G. Ecker, and A. Pich, Phys. Lett. **B304**, 347 (1993).
- [9] A. Alavi-Harati *et al.*, Phys. Rev. Lett. **83**, 917 (1999).
- [10] A. Lai *et al.*, Phys. Lett. **B536**, 229 (2002).
- [11] F. Gabbiani and G. Valencia, Phys. Rev. **D64**, 094008 (2001); Phys. Rev. **D66**, 074006 (2002).
- [12] V.V. Anisimovsky *et al.*, Phys. Rev. Lett. **93**, 031801 (2004).
- [13] M.S. Atiya *et al.*, Nucl. Instrum. Methods Phys. Res., Sect. A **279**, 180 (1989).
- [14] M.S. Atiya *et al.*, Nucl. Instrum. Methods Phys. Res., Sect. A **321**, 129 (1992).

- [15] J. Doornbos *et al.*, Nucl. Instrum. Methods Phys. Res., Sect. A **444**, 546 (2000).
- [16] E.W. Blackmore *et al.*, Nucl. Instrum. Methods Phys. Res., Sect. A **404**, 295 (1998).
- [17] I-H. Chiang *et al.*, IEEE Trans. Nucl. Sci. **42**, 394 (1995); T.K. Komatsubara *et al.*, Nucl. Instrum. Methods Phys. Res., Sect. A **404**, 315 (1998).
- [18] D.A. Bryman *et al.*, Nucl. Instrum. Methods Phys. Res., Sect. A **396**, 394 (1997).
- [19] O. Mineev *et al.*, Nucl. Instrum. methods Phys. Res., Sect. A **494**, 362 (2002).
- [20] T. Yoshioka *et al.*, IEEE Trans. Nucl. Sci. **51**, 334 (2004).
- [21] S. Adler *et al.*, Phys. Rev. **D65**, 052009 (2002).
- [22] T. Yoshioka, Ph.D. thesis, University of Tokyo, 2005.
- [23] S. Adler *et al.*, Phys. Rev. Lett. **88**, 041803 (2002); S. Adler *et al.*, Phys. Rev. Lett. **84**, 3768 (2000); S. Adler *et al.*, Phys. Rev. Lett. **79**, 2204 (1997).
- [24] G.J. Feldman and R.D. Cousins, Phys. Rev. **D57**, 3873 (1998).
- [25] E.g., J. Trampetić, hep-ph/0212309.